# Competition between fusion-evaporation and multifragmentation in central collisions in $^{58}$Ni + $^{48}$Ca reaction at 25 AMeV



2013 J. Phys.: Conf. Ser. 420 012084

(http://iopscience.iop.org/1742-6596/420/1/012084)

Journal of Physics: Conference Series **420** (2013) 012084 doi:10.1088/1742-6596/420/1/012084

# Competition between fusion-evaporation and multifragmentation in central collisions in $^{58}$Ni + $^{48}$Ca reaction at 25 AMeV

**L. Francalanza[1,2], U. Abbondanno[4], F. Amorini[1,2], S. Barlini[5], M. Bini[5], R. Bougault[6], M. Bruno[7], G. Cardella[3], G. Casini[8], M. D'Agostino[7], E. De Filippo[3], J. De Sanctis[7], E. Geraci[2,3]A. Giussani[9], F. Gramegna[10], B. Guiot[7], V. Kravchuk[10], E. La Guidara[11], G. Lanzalone[12,1], N. Le Neindre[6], C. Maiolino[1], P. Marini[7], L. Morelli[7], A. Olmi[8], A. Pagano[3], M. Papa[3], S. Piantelli[8], S. Pirrone[3], G. Politi[2,3], G. Poggi[5], F. Porto[2,1], P. Russotto[1,2], F. Rizzo[2,1], G. Vannini[7], L. Vannucci[10]**

1) INFN Laboratori Nazionali del Sud – LNS, Catania, Italy.
2) Dipartimento di Fisica, Università di Catania, Italy.
3) INFN Sezione di Catania, Italy.
4) INFN Sezione di Trieste, Italy.
5) Dipartimento di Fisica, Università di Firenze, INFN Sezione di Firenze, Italy.
6) LPC Caen, IN2P3-CNRS/ENSICAEN and Université, F-14050 Caen cedex, France.
7) Dipartimento di Fisica, Università di Bologna and INFN Sezione di Bologna, Italy.
8) INFN, Sezione di Firenze, Italy.
9) Dipartimento di Fisica, Università di Milano and INFN Sezione di Milano, Italy.
10) INFN Laboratori Nazionali di Legnaro, Italy
11) Centro Siciliano di Fisica Nucleare e Struttura della Materia, Catania, Italy.
12) Università Kore, Enna, Italy.

Email: laura.francalanza@ct.infn.it

**Abstract**. The experimental data concerning the $^{58}$Ni+$^{48}$Ca reaction at $E_{lab}$(Ni)=25A MeV, collected by the CHIMERA 4π device, have been analyzed in order to investigate the competition among different reaction mechanisms for central collisions in the Fermi energy domain. The method adopted to select such central collisions, by means of construction of the kinetic energy tensor and, consequently, the evaluation of the "flow angle" event by event is presented. Some global variables, able to characterize the pattern of central collisions, have been constructed, and the main features of the reaction products are analyzed in terms of some observable, like mass and velocity distributions, as well as their correlations. Much emphasis was devoted to the competition between fusion-evaporation processes with consequent identification of a heavy residue and multifragmentation of a well defined (if any) transient nuclear system formed in central collisions.

## 1. Introduction

Nuclear reactions induced by heavy ions in the Fermi energy domain (40 AMeV) are characterized by a transition from the mean field dissipation mechanism (one-body dissipation), dominating at bombarding energy close to the Coulomb barrier between the two interacting nuclei to the nucleon-

nucleon interacting process (two body dissipation) that is the dominant mechanism at beam energies well above the Fermi energy domain.

An experimental signature of this transition mechanism is the observation at medium energy central collisions of a copious production of Intermediate Mass Fragments (IMFs) of charge roughly in the range $3 \leq Z \leq 8$, and having intermediate velocity with respect to projectile's and target's velocity. The multiplicity of this kind of reaction products is observed to be much larger than that expected in the de-excitation of an equilibrated nuclear system produced in fusion-evaporation reactions as observed in the lower beam energy. Different scenarios have been proposed in order to explain this new multifragmentation process**.** The existing models range from prompt dynamical emissions, simulated in the contest of transport theories, to statistical multifragmentation emissions of a low density composite nuclear system at chemical equilibrium (see for instance ref.1).

Nuclear reactions in the Fermi energy domain offer unique opportunities to better understand the evolution of the many body nuclear systems under different experimental conditions. Studying multifragmentation processes as a function of impact parameter, relative kinetic energy and size of interacting ions, is important in order to disentangle different reaction mechanisms, ranging from the quasi-elastic to the most dissipative collisions. In particular, intermediate energy collisions at small impact parameters are of great interest because they allow us to study reactions where maximum transferred linear momentum and formation of single highly excited sources could be expected to occur.

## 2. The experiment

The experiment was performed by the NUCLEX-ISOSPIN collaboration and it was realized with the CHIMERA apparatus, located at LNS – INFN (Catania).

An ions beam of $^{58}$Ni was accelerated on a thin target of $^{48}$Ca by the LNS Superconducting Cyclotron, and the reaction products were collected by the 1192 Si-CsI(Tl) telescopes of CHIMERA $4\pi$ multidetector, covering almost 94% of the total solid angle [2,3]. Events were collected when at least two Silicon detectors were fired, i.e. when the charged particle multiplicity was greater than two ($M_{CP} \geq 2$).

By means of the $\Delta E$-E identification technique, it was possible to determine the atomic number Z of the reaction products punching through the silicon detector and stopped in the CsI(Tl) crystal as well as the charge and mass of those IMFs with $3 \leq Z \leq 8$, detected at laboratory angles greater than 13°; the Time-of-flight (TOF) technique provided the measure of particles' velocity, by using the cyclotron radiofrequency as start reference time, and the silicon time signal as stop.

Then, combining the energy and the TOF information, it was possible to evaluate the mass of particles stopped in the first stage of telescopes.

In this analysis the Pulse Shape Discrimination (PSD) technique, for the identification of charged light particles, has not been performed, which, however, only slightly affects the global reconstruction of the reaction pattern, made on an event-by-event basis.

## 3. Event selection

The present analysis was performed on the so called "complete events", that are those events where the total detected charge ranges between 70% and 105% of the total charge of the interacting system, as well as the total measured linear momentum (i.e. the projection of the total momentum on the beam axis) with respect to the projectile's momentum.

In this way, the 11.5% of total collected events has been selected.

In order to characterize these complete events, the correlation between the longitudinal component (i.e. along the beam axis) of the velocity, $v_{par}$, and the mass number, A, for each detected reaction product is constructed and shown in figure 1: a large number of fragments with velocity values close to projectile's velocity ($v_{proj}$ = 6.5 cm/ns) and masses around 40-45 amu are present; these fragments can be associated with projectile's remnant (PLF). Similarly, it is possible to note a relevant contribution of slow moving fragments corresponding to target's remnants. Moreover, in the middle

velocity region, centered roughly around the centre of mass velocity ($v_{CM}$ = 3.8 cm/ns), it is also present a broad component of reaction products with masses larger than projectile or target ones, reminiscent of the formation of a composite nucleus following the complete stopping of the binary interacting system.

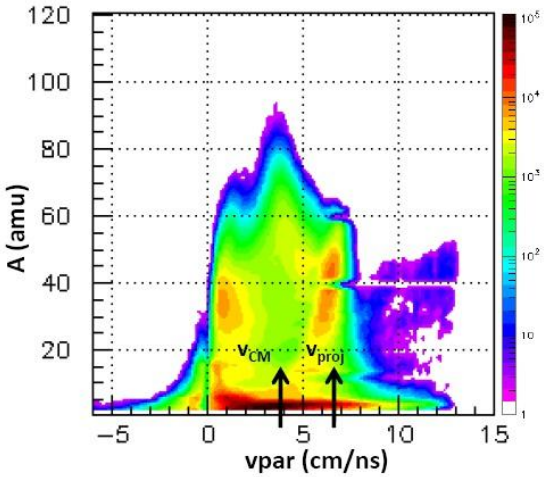


Figure 1 Correlation between the longitudinal component (i.e. along the beam axis) $v_{par}$ (cm/ns) and the mass A (amu) for all detected reaction products in complete events.

## 4. Central collisions

In order to perform a good selection of centrality, a method based on imposing several cuts on the global variable "flow angle", $\vartheta_{flow}$ , that is related to the shape of the event in momentum space, is used [4,5,6,7,8]. This latter variable is built starting from the Cartesian coordinates of the measured linear momenta, in the centre of mass frame, for all the fragments (Z≥3) detected in each event. The kinetic flow tensor, $Q_{ij}$, is built event by event as follow:

$$Q_{ij} = \sum_{Z\geq 3} {}^{p_i p_j}/_{2m} \quad (1)$$

This tensor is a generalization of the sphericity tensor, widely used in high energy particle physics and adapted to nuclear reactions in which composite fragments are produced. In its diagonal form $Q_{ij}$ defines an ellipsoid in momentum space with the three principal axes oriented along the three eigenvectors, whose corresponding eigenvalues $f_1$, $f_2$ and $f_3$, are sorted and ordered according to the inequalities $f_1 > f_2 > f_3 > 0$ [4,9,10,11,12]. The orientation of the main axis of the ellipsoid (eigenvector corresponding to $f_1$) measured with respect to the direction of the incident beam defines the flow angle $\vartheta_{flow}$.

Flow angle assumes values ranging from 0 to 90 degrees. For peripheral and semi-peripheral collisions, where the events keep memory of the binary character of the reaction, the shape is elliptic and $\vartheta_{flow}$ assumes small values, while for more central collisions a more spherical shape is predicted, so that $\vartheta_{flow}$ will assume larger values, up to 90 degrees.

Figure 2 shows the correlation plot between the Total Kinetic Energy (measured like the sum of kinetic energy of all detected fragments in each event) and the flow angle variable [13]. An increase in $\vartheta_{flow}$ values results in a selection of more dissipative collisions.

Three $\vartheta_{flow}$ windows, $\vartheta_{flow} \leq 30°$, $30° < \vartheta_{flow} \leq 60°$, $\vartheta_{flow} > 60°$, are evidenced in the Total Kinetic Energy- $\vartheta_{flow}$ tridimensional plot, as shown in figure 2. For each of these windows, in figure 3 the mass-velocity correlation plot are shown, for all reaction fragments with atomic number, $Z \geq 3$.

Following the pattern of $v_{par}$-A correlation with increasing of flow angle values, it is evident a steady decrease of PLF and TLF that is a signature of a gradual vanishing of peripheral collisions. Moreover, in the region of flow angle greater than 60 degrees, the longitudinal velocity spectrum is more and more centered on the $v_{CM}$ , and a relevant emission component due to fragments with mass

values greater than those of projectile or target, also exceeding 60 amu, is clearly observed. These events represent strong indication for the formation of a heavy residue coming from fusion-like evaporation processes.

So, in the following, we will refer to events in the third region of flow angle ($\vartheta_{flow} \geq 60°$) as central events [7], that cover the 6.2% of the complete events.

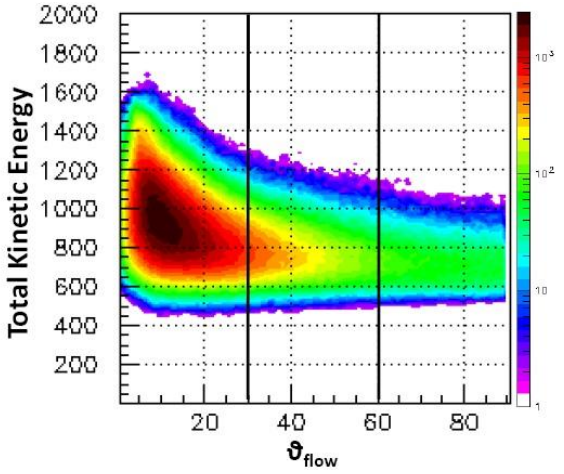


figure 2 Total Kinetic Energy (TKE) and flow angle correlation, for all the complete events.

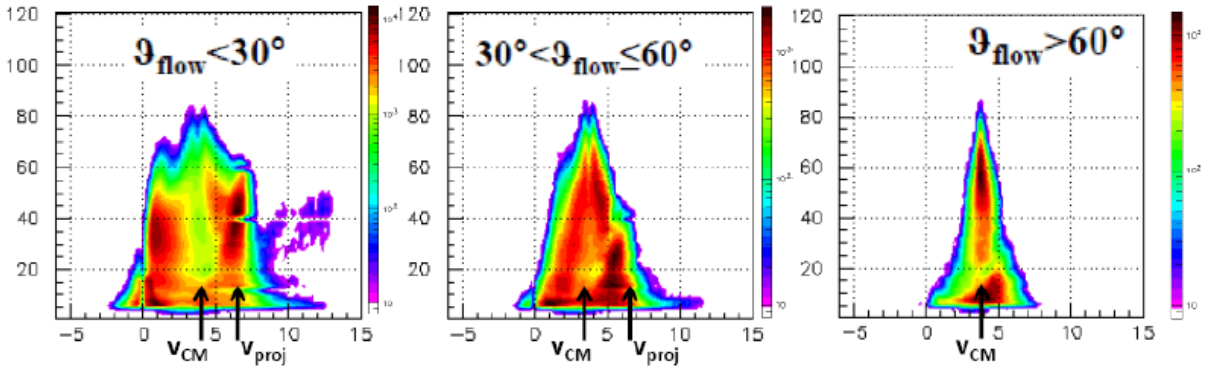


Figure 3 Correlation between parallel velocity component (cm/ns) and mass (amu) for all reaction fragments (Z≥3) in the three regions of flow angle.

*4.1. Qualitative characterization of central collisions: an event by event analysis*

In order to better characterize these central events, in figure 4 the same velocity – mass correlation plot is reported, only for the heaviest fragment emitted in each event.

In figure 4 it is possible to notice the coexistence of events where such heaviest fragment has mass around 60-70 amu, that can be related to a fusion-evaporation mechanism, and others, characterized by lower mass values of the heaviest fragment that are good candidates for a "prompt" multifragmentation process.

So, in order to disentangle between these two classes of events, we chose to impose preliminarily an arbitrary cut at mass value equal to 50 amu. In order to better characterise our choice, the mean values of IMFs with atomic number $Z \geq 3$, and light charged particles multiplicities, $\langle M_{IMF} \rangle$ and $\langle M_{LCP} \rangle$ respectively, are shown in figure 4 for both the two classes of fragments.

We see that the biggest fragment with mass 50 amu or larger is preferentially emitted as a unique heavy fragment (43.5 % of events in the upper box of figure 4) in coincidence with 4-5 light charged particles (Z=1, Z=2) or, alternatively, together with a few (1-2) light fragments; In contrast, by inspecting the lower box of figure 4, where any presence of a heavy residue is not noticed, it is seen

that the fragment multiplicity $M_{IMF}$ spans a substantially wider range of values, with a mean of $<M_{IMF}> = 3$, and reaching maximum values as high as $M_{IMF} = 6$. It has to be noted that for these latter events, the light charged particle multiplicity is lowered to a mean value of about three particles per event.

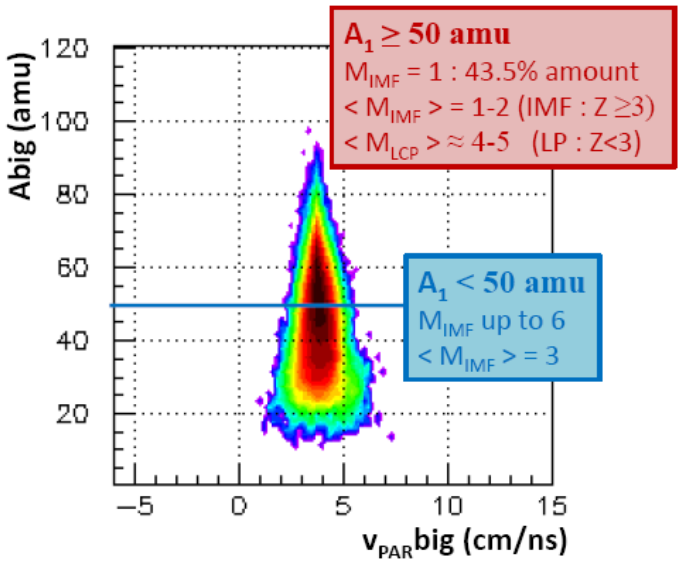


Figure 4 Mass (amu) and longitudinal velocity (cm/ns) for the heaviest fragment for central events.

These observations are strongly supported by the diagrams of figure 5, respectively for the first and the second class of above mentioned events, where three curves (color printed on line), reproduce the mass distributions of the three heaviest fragments emitted in each event (ordered according to decreasing masses). The distributions of figure 5 (left panel) display the characteristic features of typical fusion-evaporation phenomena, where the heaviest fragment is accompanied with lighter reaction products and there is a strong difference in mass value between the biggest and other emitted fragments. The distributions in the right panel of figure 5 display attributes of typical multifragmentation events characterized by a clear tendency towards the splitting of the composite system in fragments with nearly equal masses.

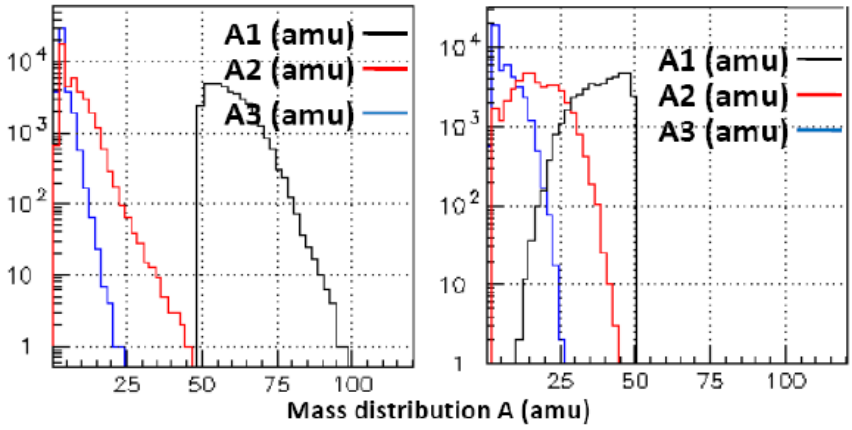


Figure 5 Left: Mass distributions of the three heavier fragments for events with a fusion-evaporation like residue (events in upper box of figure 4); Right: the same distributions for multifragmentation-like events (in lower box of figure 4). Different colors (see the web version of the paper) correspond to different types of fragments: the heaviest, the second and the third massive fragment, according to decreasing mass values.

*4.2. Comparisons with calculations*

We have compared mass distributions and multiplicities for selected central events (without any differentiation among fusion-evaporation and multifragmentation like events) with those predicted by a two step mechanism: dynamical stochastic BNV calculation followed by the sequential de-excitation of a composite source (SIMON code) [14]. The source information was obtained from BNV calculation, including pre-equilibrium emission, and corresponds to a source with mass equal 94 amu, a source's charge of atomic number Z =43 and an excitation energy equal to 400 MeV (±50MeV). In this calculations we have considered events from central collisions of vanishing angular momentum (L=0).

Figure 6 shows the comparison between fragment multiplicity distributions (left panel) and between mass distributions (right panel) for experimental data (black line) and for the calculations (red line. At this stage of comparison the simulation data are not yet filtered, i.e., energy and mass resolutions, detector efficiency and trigger threshold are not included. We can notice the quite good agreement in reproducing the shape of both multiplicity and mass distribution for both heavy and light reaction products. Moreover, in figure 7 the same analysis is constructed, but considering the mass distribution only of the heaviest residue in such central events: the same consideration mentioned above about the filter on experimental data is still valid.

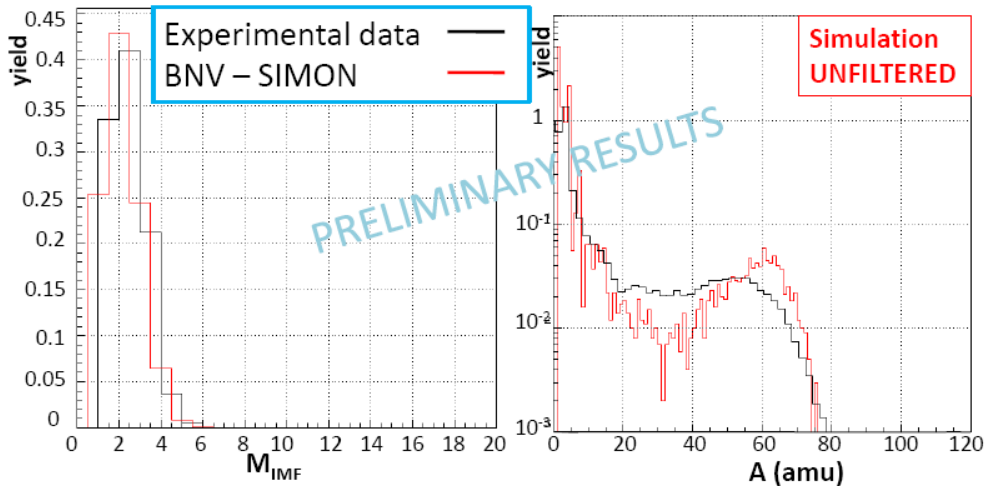


Figure 6 left: Comparison between experimental (black line) and theoretical (red line) $M_{IMF}$ distribution. Right: mass distribution for experimental data (black line) and results of calculation (red line).

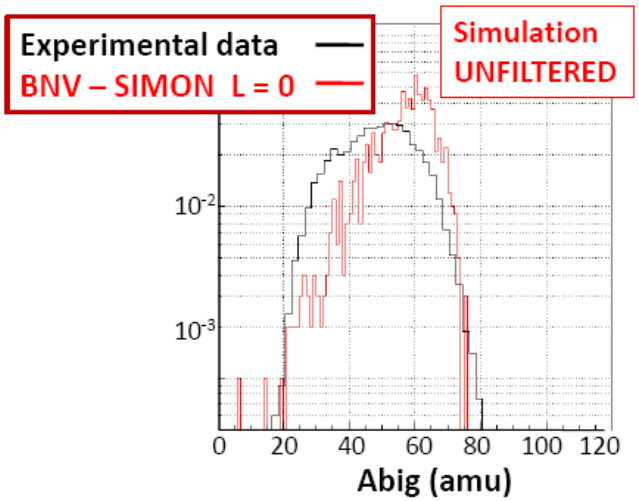


Figure 7 Mass distributions for the heavy residue: experimental data in black and theoretical calculations in red.

## 5. Conclusions

The experimental data of $^{58}$Ni+$^{48}$Ca reactions at $E_{lab}$(Ni)=25A MeV, collected by using the CHIMERA 4π device, have been analyzed in order to investigate the competition among different reaction mechanisms for central collisions.

As main criterion for centrality selection we have chosen the flow angle method, making an event-by-event analysis that considers the shape of events in the momentum space. For the selected central events ($\vartheta_{flow}$>60°), mass-velocity correlations, built for all emitted fragments show, besides the component with mass number A < 20, the presence of a broad component centered at $v_{CM}$ and with high values of mass, strongly indicating a heavy residue from a composite source.

By means of further analysis concerning the multiplicity of fragments ($M_{IMF}$) and of charged light particles ($M_{LCP}$), and the mass distribution of the heaviest fragment emitted in such selected central collisions, a clear signature for the coexistence of two different reaction mechanisms is evident: a fusion-evaporation process, associated with events with low $M_{IMF}$ and relevant differences in mass distributions of emitted fragment, and a multifragmentation like mechanism, related to higher fragment multiplicity values and similar mass values for the correlated fragments in each event.

Preliminary comparisons of experiment with reaction simulations show reasonable qualitative agreement with the assumption of sequential multifragmentation emission.

However further analysis and new information (as for instance IMF-IMF angular correlations distribution, statistical multifragmentation model calculations..) are needed in order to obtain definitive conclusions about the nature of the multifragmentation process of the composite system in a large number of light fragments of similar mass.

## 6. Acknowledgments

Authors are grateful to Maria Colonna of LNS in Catania for providing them the stochastic BNV calculations and for invaluable discussions.

## 7. References

[1] W. G. Lynch, Nucl. Phys. A583 (1995) 471-480
[2] A.Pagano et al., Nucl. Phys. A 734 504 (2004).
[3] A.Pagano for CHIMERA Collaboration: *Proposal for upgrading CHIMERA 4π detector,* Proceeding XLII International Winter Meeting on Nuclear Physis, Bormio (pp. 150-155) – Italy, March 2005.
[4] J. Cugnon et al., Nucl. Phys. A 397 519-543 (1983).
[5] E. Geraci et al., Proceeding Of The IWM2009, International Workshop on Multifragmentation and related topics, Catania (pp. 30-36) – Italy, November 2009;
NPA 732 (2004) 173.
[6] L. Francalanza, "Central collisions in $^{58}$Ni + $^{48}$Ca system with CHIMERA at 25 AMeV", Il Nuovo Cimento, DOI 10.1393/ncc/i2012-11305-7 (2012).
[7] N. Marie et al., Phys. Lett. B391 (1997) 15.
[8] M. D'Agostino et al., Phys. Lett B368 (1996) 259.
[9] M. Gyulassy et al., Phys. Lett. vol. 110B, number 3,4 (1982).
[10] Herrman et al., Annu. Rev. Nucl. Part. Sci. 1999. 49:581–632 (1999).
[11] H. Stocker et al., Nucl. Phys. A 387 205c-218c (1982).
[12] H. Stocker and W. Greiner, Phys. Rep.137 277-392 (1986).
[13] J. F. Lecolley et al., Phys. Lett B 387 460 (1996).
[14] D. Durand, Nucl. Phys. A541, 266 (1992).